2022 19th International Conference on Electrical Engineering, Computing Science and Automatic Control (CCE). Mexico City, Mexico. November 9-11, 2022

Space Weather observations and HF transmissions around the 2021 autumn equinox

Giselle M. Galvan-Tejada
Department of Electrical Engineering, Communications Section
Center for Research and Advanced Studies of National Polytechnic Institute
Mexico City, Mexico
0000-0002-0674-3425

Miguel Herraiz-Sarachaga
Department Physics of the Earth and Astrophysics
Complutense University of Madrid
Madrid, Spain
0000-0002-0793-7117

Mario A. Mendoza-Barcenas
Aerospace Development Center
National Polytechnic Institute
Mexico City, Mexico
0000-0001-9872-5349

Zian Aguirre
National Emergency Network
Mexican Federation of Radioexperimenters
Colima, Mexico
zianjulio@gmail.com

***Abstract*— Continuing the study of the influence of Space Weather conditions on radio communications in Mexico accomplished for 17 days of the spring of 2020, results of a longer campaign and around autumn of 2021 are analyzed in this paper. The length of the study and the number and variety of people collaborating in its development turn this new experiment into a remarkable event of citizen science. While the Space Weather conditions of the study in 2020 corresponded to an early stage of the Cycle 25 characterized by a very low level of solar activity, in the 77 days of the new observation period, 8 M class and 1 X class Solar Flares and 17 Coronal Mass Ejections took place. In addition, Coronal Holes were present in 50 days. This significant activity originated 2 G1, 1 G2 and 2 G3 geomagnetic storms and increased the scientific interest of the survey. This article includes a short explanation of the main solar phenomena affecting Space Weather and their presence in the survey followed by the description of the main variations of radio signals recorded by radio ham operators of the National Emergency Network in Mexico, at 7.120 MHz (40 m band) and 3.720 MHz (80 m band) frequencies. According to the records, the first band seems to present better response to propagation conditions than the second one during the experiment period, but a larger amount of observations are necessary to confirm this result.**

Keywords—HF radio communications; Space Weather; Radio Wave Propagation Conditions.

I. INTRODUCTION

The effects of solar phenomena on radio communications have been studied for long time. For example, recently Muratore et al. [1] have shown how solar activity affected the performance of a mobile communications operator whose principal function is to control base stations at the 2.6 GHz band in Italy. Another example is the long-range high frequency (HF) communication operating at 3-30 MHz around the world whose main propagation medium is the ionosphere, which is well known to be related to different solar emissions [2] and therefore varies as a function of the season and time of day among others. In this context, the equinox periods have a peculiar interest because ultraviolet (UV) radiation introduced to the ionosphere could achieve to have radio communication links between both hemispheres for longer periods of the day at some HF bands [3]. As an example of this phenomenon, an analysis of Space Weather events and how radio amateur operations were affected around the 2017 autumnal equinox in several regions of the world was presented in [4].

Considering the planning requirements and the tendency of the seasonal distribution of geomagnetic storms to reach higher values at equinoxes [5-7], the campaign was planned around the 2021 autumn equinox in the northern hemisphere. It started in August 23 and ended in November 17 and counted on the collaboration of more than 100 amateur radio operators.

The tracking of Space Weather variations and their effect on Earth was done by the daily consideration of 14 different phenomena and parameters. Seven of them describe the solar activity: Sunspot and Active Regions numbers; Solar Flares characteristics; Coronal Mass Ejections, CMEs, and Radio emissions occurrence; presence of Coronal Holes, and value of F10.7 cm radio emissions. The solar wind was evaluated paying attention to Speed, Particle Density, total Interplanetary Magnetic Field, B_T, and its vertical component, Bz. Finally, the impact on Earth was estimated considering the Geomagnetic Equatorial Disturbance Storm-Time index, Dst, the Planetary K index, Kp, and the occurrence of Geomagnetic Storms. Most information was taken from: weatherspace.com; https://www.swpc.noaa.gov/ https://omniweb.gsfc.nasa.gov/;

https://wdc.kugi.kyoto-u.ac.jp/; and

http://www.sciesmex.unam.mx/.

In terms of radio communications parameters, a set of analogue signals recorded by radio ham operators of the National Emergency Network (RNE for its acronym in Spanish) in Mexico was taken as basis of analysis for our study. In addition, the probability to have favorable propagation conditions for different HF bands was also considered to analyze the temporal changes into the signals reported by the members of the RNE. This probability was obtained from the well-known open online software VOACAP (https://www.voacap.com/hf/) widely recognized by the scientific community.

Thus, the rest of the paper is organized as followed: Section II presents an outline of main solar phenomena that affect Space Weather parameters and their presence during the study period; Section III details the experimental settings of radio ham communications and the analysis of observations reported by radio ham operations and some radio propagation considerations are exposed in Sections IV and V, respectively. Finally, concluding remarks are given in Section VI.

978-1-6654-5508-4/22/$31.00 ©2022 IEEE

II. Solar Phenomena affecting Space Weather

The presence of Solar Flares alerts about the sudden increases of electromagnetic radiation that can rise the electronic density of the ionospheric D region and its capacity to absorb signals at the HF band of the radio spectrum. This process can produce radio blackouts in the 5-30 MHz frequency range. As the X-ray and solar radio frequency emissions (known as radio bursts) travel at light speed, their effects on the ionosphere take place about 8 minutes later than their origin. The absorption rise in the D layer also explains the Lowest Usable Frequency (LUF) increase in periods or circumstances of high solar activity. At night the D layer disappears but the F2 region remains and can be affected by the effect of ionospheric storms several days after the occurrence of the solar energetic event. So, the perturbed F2 layer can cause a decrease in the Maximum Usable Frequency (MUF) and produce anomalous HF transmission. Some other ionospheric phenomena such as the appearance of Transient Ionospheric Disturbances (TIDs), bubbles or spread-F can also affect the HF transmission at night time.

As the X-ray and solar radio frequency emissions (known as radio bursts) travel at light speed, their effects on the ionosphere take place about 8 minutes later than their origin. The presence of radio bursts known as Type II and IV emissions have also been included in the survey. These solar radio bursts are temporary and intense increases of emissivity in the solar radio dynamic spectrum. Radio Emissions Type II are considered as bursts excited by magnetohydrodynamics (MHD) shocks in the solar atmosphere and are closely related to solar flares and high velocity coronal ejections [8]. A radio emission Type IV is the broadband continuum emission in metric wavelength that usually lasts for a relatively long time (>10 minutes) [9] and therefore could have a non-negligible impact on radio communications.

Large solar flares also can originate Solar Proton events characterized by the ejection in the solar wind of accelerated charged particles, mainly protons, with very high velocities. The most energetic protons can take only a few tens of minutes to reach the Earth. They can penetrate the magnetosphere, strike the atmosphere in high latitudes, and cause shortwave radio fades and many problems to satellites, electronic devices, and even biological processes.

The presence of CMEs and Coronal Holes opens the possibility of geomagnetic storms whose probability can be evaluated considering the characteristics of the present solar wind and, in the case of CMEs, the size and position of the involved active region. Coronal Mass Ejections are giant emissions of solar coronal mass (thousands of millions of tons) that drag the solar magnetic field “frozen” within. This emission moves with velocity varying between 250 y 3000 km/s and modifies all solar wind characteristics. It takes between 1-3 days and 15-18 hours to reach our planet. CMEs carry enormous amounts of high energy and particles and are the main responsible for geomagnetic storms that can damage spacecrafts and satellites and weaken short radio communication waves.

Flares and Coronal Mass Ejections are often accompanied by accelerated electrons that can in turn emit radiation at radio wavelengths. As mentioned above, this radiation is observed as solar radio bursts. Type II emissions exhibit a relatively slow drift from high to low frequencies of around 1 MHz per second, typically over the course of a few minutes Type II bursts are produced at the leading edge of a CME, where a shock wave accelerates the electrons responsible for stimulating plasma emission [10]. The emission mechanism for Type IV bursts is generally attributed to gyrosynchrotron emission, plasma emission, or some combination of both that results from fast-moving electrons trapped within the magnetic fields of an erupting CME [11].

Coronal Holes are coronal regions that appear dark in extreme violet or X-ray images. These zones, less dense and cooler than their surroundings, present open magnetic field lines that inject heated coronal plasma into the solar wind, increasing its speed. They are the principal source of geomagnetic storms at periods of low solar activity.

During the campaign occurred 8 M class and 1 X class Solar Flares, and 17 CMEs. In addition, Coronal Holes were present in 50 out of the 77days. These observations are the basis for the selection of solar active days showed in Table I.

Indices Dst and Kp inform about the present geomagnetic conditions on Earth. The first one is measured in nT units and evaluates the intensity of the globally symmetrical equatorial electrojet (the "ring current"). It takes negative values and when an intense geomagnetic storm takes place, Dst varies between -100 and -249 nT [12]. A Dst value lower than -30 nT is usually considered as the beginning of a perturbed magnetic situation. In turn, Kp index measures the global magnetic disturbance and Kp = 4 indicates the start of the global magnetic perturbation.

The analysis of this set of data allows to classify the days according to their Space Weather characteristics or considering the geomagnetic perturbation on Earth. In the first case the criterion has been the simultaneous presence of at least 3 of the following phenomena: occurrence of C3 (or higher) Solar Flares, CMEs or radio bursts, and the presence of Coronal Holes. In the second case, attention has been paid to Dst and Kp indices to select the days geomagnetically perturbed. The result of the first selection is shown in Table I, whereas Table II lists the results obtained in the second search. The joint consideration of both sets of days helps to select the dates of the campaign with the higher possibility to present radio waves transmission anomalies.

It is worth remembering the occurrence during the survey of two G1 storms (on 17 September and 31 October), one G2 (on October 12) and two G3 (on November 3 and 4). As can be noted, solar activity, and consequently Space Weather, were far different from those recorded during the preliminary study made in 2020 by [13].

TABLE I. MOST INTERESTING DAYS CONSIDERING 4 CHARACTERISTICS OF THE SPACE WEATHER.

Day	Strongest Solar Flare	Occurrence of CMEs	Occurrence of Radio Emissions	Presence of Coronal Holes
August 24	C4	YES	YES	YES
August 28	M4.7	NO	YES	YES
September 8	C8	YES	YES	NO
September 17	C3	YES	YES	NO
September 23	M3.2	YES	YES	YES
September 28	C1.6	YES	YES	YES
October 9	M1.6	YES	YES	NO
October 26	M1	YES	YES	NO
October 28	X.1	YES	YES	NO
November 1	M1	YES	YES	NO
November 2	M1.7	YES	YES	NO
November 9	M2	NO	YES	NO

TABLE II. DAYS WITH GEOMAGNETIC PERTURBATION ON EARTH

Day	Maximum Kp Index	Minimum Dst Index (nT)
August 28	4	-74
September 17	5	-77
September 22	4	-32
October 1	4	-32
October 2	4	-30
October 12	6	-52
October 17	4	-39
October 18	4	-43
October 31	5	-36
November 2	4	-30
November 3	4	-32
November 4	7	-115
November 5	4	-55
November 6	4	-47
November 7	4	-38

III. RADIO HAM EXPERIMENTAL SETTINGS

In order to consider the autumn equinox in the northern hemisphere, the experiment was conducted from August 25 to November 17, 2021. We recorded the information provided by radio ham operators of the National Emergency Network (RNE for its acronym in Spanish) of the Mexican Federation of Radio Hams (FMRE for its acronym in Spanish). This network conducts testing practices over Mexico during approximately 30 minutes every night of the year (around 21:00 hrs. Local Time) for the RNE purposes. A radio ham station is selected each day from a pool of qualified stations to operate as control station whereas the other radio ham stations operate as nodes of the control station. The transmissions were carried out at two HF frequencies: 7.120 MHz (40 m band) and 3.720 MHz (80 m band) using analogue single sideband (SSB) modulation format. Fig. 1 shows an example of nodes of the RNE transmitting at the 40 m band towards the control station XE1ATZ on October 9, 2021.

Signals transmitted to the control station are registered from two numbers, the readability (R) and the signal strength (S), so forming what is known as RS levels. Table III shows the meaning of these levels. For example, RS=59 corresponds to a perfectly readable and extremely strong signal, RS=33 implies a readable with considerable difficulty weak signal, and so on.

IV. ANALYSIS OF RS OBSERVATIONS

Results of the RS levels reported by the RNE radio ham operators help us to analyze the HF communications performance. It is important to point out that the periodic operation of the testing practices of the RNE allows having a fair comparison from one day to another one. We select the XE1ATZ control station, which reported the most contacts obtained through the observation period (11 days for the 40 m band and 27 days for the 80 m band). In order to compare the RS levels for different days, we consider only those stations that were reported at least twice.

Fig. 2 shows the RS levels reported by radio ham stations at 40 m band, where most transmissions were concentrated on September 9 and 23. As can be seen, a general trend of RS=59 is reported for most of stations. However, we found some stations which presented lower and variable RS levels, such as the XE3ARL station with RS=39 (September 9), RS=33 (September 23), and RS=48 (October 9), three days with occurrence of Solar Flares. In turn, the XE2LSM station reported an interesting change on October 14 with an RS=39, two days after a significant geomagnetic activity (Kp=6 and G2 storm) on October 12. Previous days (September 9, September 23, October 9), almost 10 days later (October 23), and even on the same day (October 12), this station had an RS=59. Fig. 3 shows the RS levels for the 80 m band for the 27 days distributed along the observation period (see Table IV for dates of records).

TABLE III. RS LEVELS (http://www.arrl.org/quick-reference-operating-aids)

Readability (R)		Signal Strength (S)		Signal Strength (S)	
1	Unreadable	1	Faint signals, barely perceptible	6	Good signals
2	Barely readable	2	Very weak signals	7	Moderately strong signals
3	Readable with considerable difficulty	3	Weak signals	8	Strong signals
4	Readable with practically no difficulty	4	Fair signals	9	Extremely strong signals
5	Perfectly readable	5	Fairly good signals		

TABLE IV. DATES OF THE OBSERVATIONS AT THE 80 M BAND

Day	Date	Day	Date
1	28/08/2021	15	29/09/2021
2	31/08/2021	16	01/10/2021
3	02/09/2021	17	13/10/2021
4	03/09/2021	18	15/10/2021
5	06/09/2021	19	22/10/2021
6	08/09/2021	20	23/10/2021
7	15/09/2021	21	27/10/2021
8	17/09/2021	22	29/10/2021
9	18/09/2021	23	04/11/2021
10	21/09/2021	24	05/11/2021
11	22/09/2021	25	12/11/2021
12	23/09/2021	26	13/11/2021
13	24/09/2021	27	17/11/2021
14	25/09/2021		

Fig. 1 Example of RNE radio links on October 9, 2021 at 40 m band.

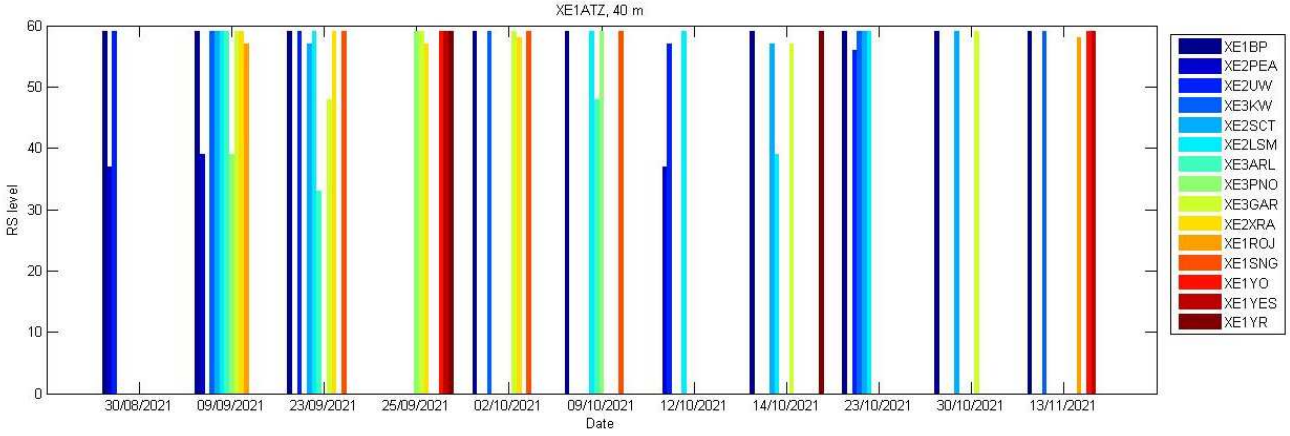

Fig 2. RS levels resulting on the 40 m band

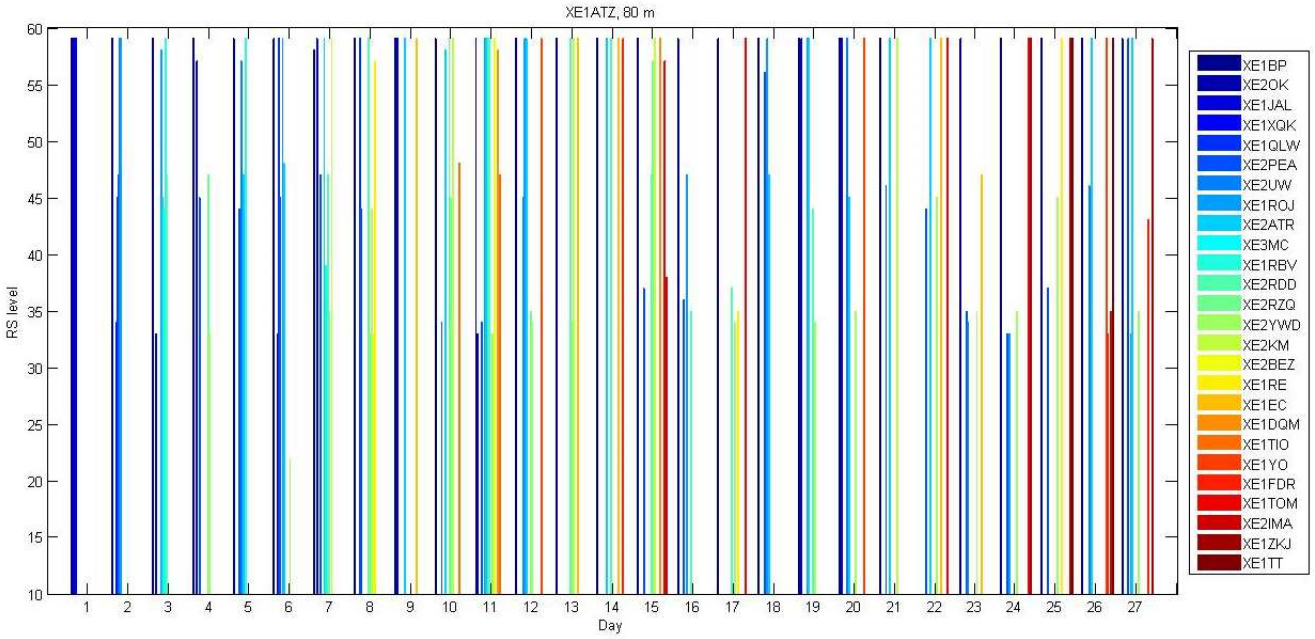

Fig. 3. RS levels resulting on the 80 m band. See Table IV for the equivalence between numbers and dates

As can be seen, there is a relatively uniform distribution of transmissions through the observation period, mainly near of the equinox period (numbers 10-11 of the horizontal-axis). However, in contrast with results of Fig. 3, we observe more variation in the RS levels for more stations. For example, the XE2RZQ station showed the following results:

- RS=47 (September 3)
- RS=35 (September 15)
- RS=33 (September 17)
- RS=45 (September 21)
- RS=35 (September 23)
- RS=57 (September 29).

Another interesting example is the XE2PEA station which had also variable RS levels:

- RS=47 (August 31)
- RS=45 (September 3)
- RS=44 (September 6)
- RS=45 (September 8)
- RS=47 (September 15)
- RS=44 (September 17)
- RS=34 (September 21)
- RS=34 (September 22)
- RS=37 (September 29)
- RS=36 (October 1)
- RS=56 (October 15)
- RS=46 (October 27)
- RS=44 (October 29)
- RS=35 (November 4)
- RS=33 (November 5)
- RS=37 (November 12)
- RS=59 (November 17).

In this last case, it can be seen a clear reduction of the RS levels around the autumn equinox and a major variability some weeks later. As was shown in Tables I and II, solar flares activity, radio emissions, and significant geomagnetic level were observed in those days. Numbers 17, 23 and 24 of the x-axis deserve special attention. Number 17 corresponds to October 13, a day with the ionosphere still affected by the G2 storm occurred the previous day. Numbers 23 and 24 stand for November 4 and 5, respectively. The first of them experimented a G3 storm with Kp = 7 and Dst = -115 nT. The second one also had a significant level of magnetic perturbation (Dst = -55 nT and Kp = 4) that could contribute to keep the ionosphere unsettled and affect the HF transmissions.

V. Comments on HF Propagation Conditions

It is well known that the ionospheric propagation can be different from one day to another one as explains in [13], which allows or not the transmission over different HF bands. Different prediction models for the ionospheric communication channel have been reported for several years as is well outlined in [14]. Moreover, artificial intelligence is currently expanding this research area [15].

In order to have a reference for the experiment period, we have selected the VOACAP model because it is able even to predict the reception of weak signals [16]. Thus, some propagation prediction graphs were generated using the online software VOACAP (https://www.voacap.com/hf/) for SSB modulation format, transmission power of 100 W and 40 m dipole antennas. Fig. 4 shows two examples of these graphs for August 31 and September 24, 2021, considering a couple radio ham stations located at grids DK89DF and EK87MX. As can be appreciated, more probabilities of favorable propagation conditions were predicted for September 24 in comparison to August 31.

Similar graphs were generated using the same settings and for those days that radio ham stations were reported to the control station. From these graphs, we gathered the probabilities values for the 40 m and 80 m bands, which are depicted in plots of Fig. 5. In this figure we are including the mean value (μ) and standard deviation (σ) for each case.

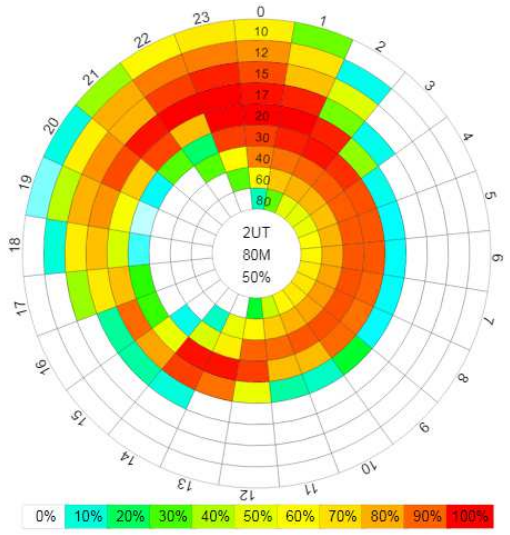

a)

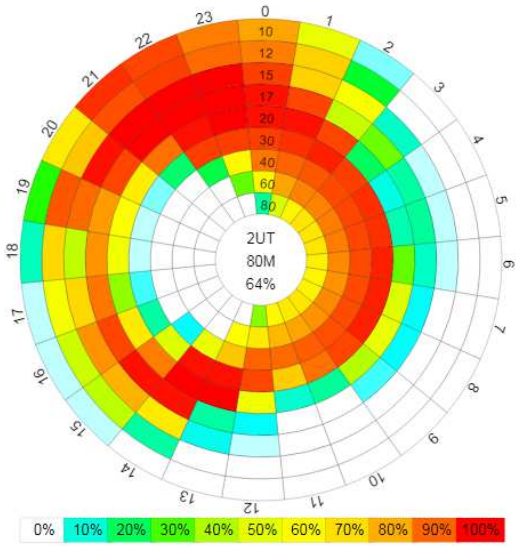

b)

Fig. 4. Probability (%) of favorable propagation conditions for HF bands, (a) August 31, 2021, (b) September 24, 2021.

As can be seen, both bands presented very low variation during days reported by radio ham operators. In terms of mean values, clearly the 40 m band presented a better probability of favorable propagation conditions in comparison to the 80 m band. The lower probability of the 80 m band explains the more variability of RS levels observed in some stations as discussed in previous section.

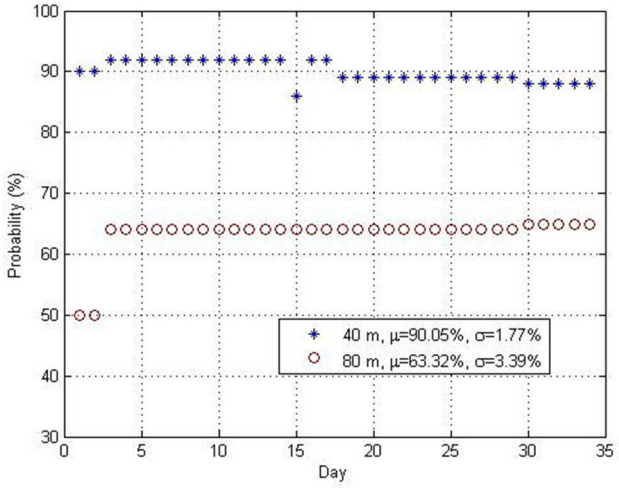

Fig. 5. Probability of having favorable propagation conditions for the 40 and 80 m bands.

VI. Conclusions

As a part of the research about space weather and radio frequency communications initiated in May-June 2020, results of observations both of parameters of solar activity (and consequent Space Weather) and radio ham transmissions at HF are reported in this paper. Particularly, these results are based on observations provided by radio ham operators, members of the National Emergency Network who conducted an experiment around 2021 autumn equinox in the northern hemisphere. New interesting Space Weather situations are pointed out, and we found some variations of RS levels reported by some radio ham stations operating in SSB mode, mainly after the equinox date. Propagation conditions given by an open website are also analyzed which demonstrate differences between HF bands and provide insights of the behavior given by several radio ham stations during the experiment period. The scarce number of available observations, especially in 40 m transmissions, prevent us from drawing well-founded relationships between detected space weather phenomena and observed radio anomalies. In a forthcoming article, results for digital radio ham signals will be reported, reinforcement the basis for a future correlation between Space Weather and performance of communications in the band of radio ham.

Acknowledgment

Authors want to thank the members of the RNE of the FMRE, Mexico, who participated during the observation period of this study. Additionally, our recognition to M. I. Rafael Prieto-Meléndez, academic of ICAT-UNAM for his unvaluable support in organizing the data of radio ham stations participating during the study.

REFERENCES

[1] G. Muratore, T. Giannini and D. Micheli, "Solar radio emission as a disturbance of radiomobile networks," Scientific Reports, vol. 12, no. 9324, pp. 1–13, 2022, doi:10.1038/s41598-022-13358-z.

[2] L. Liu, W. Wan, Y. Chen, and H. Le, "Solar activity effects of the ionosphere: a brief review," Chinese Science Bulletin, vol. 56, no. 12, pp. 1202–1211, 2011, doi: 10.1007/s11434-010-4226-9.

[3] W. Silver, "HF Propagation at the Equinox," On All Bands, September 3, 2021, https://www.onallbands.com/hf-propagation-at-the-equinox

[4] N. A, Frissell, et al., "High-frequency communications response to solar activity in September 2017 as observed by amateur radio networks," Space Weather, vol. 17, pp. 118–132, 2019, doi: 10.1029/2018SW002008.

[5] J. Bartels, "Terrestrial-magnetic activity and its relations to solar phenomena," Terrestrial Magnetism and Atmospheric Electricity, vol. 37, no. 1, pp. 1–52, 1932, doi:10.1029/TE037i001p0000.

[6] W. D. Gonzalez, E. Echer, A. L. Clúa de Gonzalez, B. T. Tsurutani, and G. S. Lakhina, "Extreme geomagnetic storms, recent Gleissberg cycles and space era-superintense storms," Journal of Atmospheric and Solar-Terrestrial Physics, vol. 73, no. 11, pp. 1447–1453, 2011, doi: 10.1016/j.jastp.2010.07.02.

[7] G. A. Mansilla, "Solar cycle and seasonal distribution of geomagnetic storms with sudden commencement," Earth Science Research, vol. 3, no. 1, pp. 50–55, 2014, doi:10.5539/esr.v3n1p50.

[8] S. Ma and H. Chen, "Two successive Type II radio bursts associated with B-class flares and slow CMEs," Frontiers in Astronomy and Space Sciences, vol. 7, no. 17, pp. 1–13, 2020, doi: 10.3389/fspas.2020.00017.

[9] M. Pick, "Observations of radio continua and terminology," Solar Physics, vol. 104, pp. 19–32, 1986.

[10] P. A. Sturrock, "Spectral characteristics of Type II solar radio bursts," Nature, vol. 192, pp. 58, 1961, doi:10.1038/192058a0.

[11] A. Boischot and J. W. Warwick, "Radio emission following the flare of August 22, 1958," Journal of Geophysical Research, vol. 64, no. 6, pp. 683–684, 1959, doi:10.1029/jz064i006p00683.

[12] D. Knipp, Understanding Space Weather and the physics behind it. Boston: McGraw Hill, 2011.

[13] M. A. Mendoza-Barcenas, G. M. Galvan-Tejada, O. Alvarez-Cardenas, M. Herraiz-Sarachaga, and A. Tamez-Rodriguez, "Preliminary study of Space Weather effects on the HF and VHF communications at low latitudes during an early stage of the solar cycle 25," 2020 17th International Conference on Electrical Engineering, Computing Science and Automatic Control (CCE) Mexico City, Mexico. November 11-13, 2020.

[14] S. G. Tanyer and C. B. Erol, "Comparison of the current methods for coverage area prediction for communication in the HF band," IEEE Antennas and Propagation Society International Symposium, vol. 4, pp. 1888–1891, 1998 [Digest. Antennas: Gateways to the Global Network. Held in conjunction with: USNC/URSI National Radio Science Meeting 1998], doi: 10.1109/APS.1998.701572.

[15] R. Buckley and W. N. Furman, "Application of machine learning techniques to HF propagation prediction," MILCOM 2021–2021 IEEE Military Communications Conference (MILCOM), pp. 623–628, 2021, doi: 10.1109/MILCOM52596.2021.9653108.

[16] J. Machado Fernández, Y. Rodríguez, Y. Vázquez, and D. Rosich, "Estimation of frequencies for National Shortwave Network with automatic link establishment equipment," Journal of Tropical Engineering, vol. 26, pp. 79–91, 2016, doi:10.15517/jte.v26i2.21519.